

# Slow Proton Exchange in Aqueous Solution. Consequences of Protonation and Hydration within the Central Cavity of Preyssler Anion Derivatives, $[|M(H_2O)|\supset P_5W_{30}O_{110}]^{n-}$

Kee-Chan Kim,<sup>1</sup> Michael T. Pope,\* Gennaro J. Gama,<sup>†</sup> and Michael H. Dickman

Contribution from the Department of Chemistry, Box 571227, Georgetown University, Washington, D.C. 20057-1227

Received June 21, 1999

**Abstract:** Redetermination of the crystal structure of the ammonium salt of the Preyssler anion,  $[NaP_5W_{30}O_{110}]^{14-}$  (**Na**), at low temperature, reveals that a water molecule is coordinated to the encrypted (sodium) cation, a feature that had been previously observed in structures of normal and acid salts of the europium(III) derivatives (**Eu** and **HEu**) and the normal salt of the uranium(IV) derivative (**U**). The crystal structures of  $(NH_4)_{13}[Ca(H_2O)P_5W_{30}O_{110}] \cdot 35H_2O$  (**Ca**),  $K_6H_7[Ca(H_2O)P_5W_{30}O_{110}] \cdot 45H_2O$  (**HCa**),  $(NH_4)_{12}[Y(H_2O)P_5W_{30}O_{110}] \cdot 30H_2O$  (**Y**),  $K_6H_6[Y(H_2O)P_5W_{30}O_{110}] \cdot 40H_2O$  (**HY**), and  $K_6H_5[U(H_2O)P_5W_{30}O_{110}] \cdot 30H_2O$  (**HU**) have also been determined. The structures reveal that the encrypted cations become more displaced from the equator of the anion as the charge of the cation increases. Evidence that these heteropolyanions can be protonated *inside* the central cylindrical cavity is provided by observation of two  $^{31}P$  NMR lines, one in acidic and one in less acidic solution. At intermediate acidities both lines are observed, indicating that proton exchange involving the internal proton is slow on the NMR time scale. The relative intensities of the two lines for the europium derivative as a function of pH could be fitted to a simple acid–base equilibrium expression. The internal water molecule of the unprotonated anion undergoes slow H/D exchange with solvent water. Isotopomers with internal HOH, HOD, and DOD are readily distinguished by P NMR (and for the first two, by H NMR) especially for derivatives with paramagnetic internal cations (Eu, U). The exchange reaction followed by  $^1H$  and  $^{31}P$  NMR in pure  $D_2O$  (pD 3.6) for the europium derivative at room temperature followed an **A**  $\rightarrow$  **B**  $\rightarrow$  **C** consecutive mechanism with effective rate constants  $k_1(HOH \rightarrow HOD) = (4.1 \pm 0.2) \times 10^{-4} s^{-1}$  and  $k_2(HOD \rightarrow DOD) = (3.4 \pm 0.2) \times 10^{-4} s^{-1}$ . The rates increased as the pH was lowered, while the rate decreased to a limit of no observable exchange at pH 7. Hydrothermal treatment of the sodium derivative in strongly acidic solutions ( $>2 M HCl$ ) releases the encrypted cation, according to  $^{31}P$  and  $^{183}W$  NMR spectroscopy and measurement of sodium activity released.

## Introduction

The remarkably robust heteropoly tungstophosphate anion, which was first described by Preyssler<sup>1</sup> as a  $P_5W_{18}$  species, was later reexamined by Alizadeh et al.<sup>2</sup> and shown by single-crystal structure analysis to be  $[NaP_5W_{30}O_{110}]^{14-}$ . The presence of a tightly encrypted sodium cation, which lies on the principal axis but not in the equatorial plane of the doughnut-shaped structure, reduces the overall virtual symmetry of the anion from  $D_{5h}$  to  $C_{5v}$ . The integrity and nonlability of the structure in solution was confirmed by  $^{23}Na$ ,  $^{31}P$ , and  $^{183}W$  NMR spectroscopy. Subsequent work<sup>4</sup> has demonstrated that, under vigorous hydrothermal conditions, the internal sodium ion could be replaced with numerous other cations of similar size such as  $Ca^{2+}$ ,  $Y^{3+}$ ,  $Bi^{3+}$ , most trivalent lanthanides, and tetravalent actinides (Th through Cm), and we have since been evaluating this chemistry with reference to the separation of species present in nuclear wastes.

<sup>†</sup> Current address: Department of Chemistry, University of Pennsylvania, Philadelphia, PA 19104.

(1) Taken from the Ph.D. Thesis of K.C.K., Georgetown University, 1998.

(2) Preyssler, C. *Bull. Soc. Chim. Fr.* **1970**, 30.

(3) Alizadeh, M. H.; Harmalkar, S. P.; Jeannin, Y.; Martin-Frère, J.; Pope, M. T. *J. Am. Chem. Soc.* **1985**, *107*, 2662.

(4) (a) Creaser, I.; Heckel, M.; Neitz, R. J.; Pope, M. T. *Inorg. Chem.* **1993**, *32*, 1573. (b) Antonio, M. R.; Williams, C. W.; Soderholm, L. J. *Alloys Compd.* **1998**, *271–273*, 846.

Soderholm et al. have reported that reaction of the Preyssler anion with  $Eu^{3+}$  yielded a product in which the lanthanide cation occupied one of two sites (A and B) that could be distinguished by fluorescence spectroscopy.<sup>5</sup> Occupation of site B was observed when  $>1$  equiv of Eu was used in sample preparation. On the basis of the different fluorescence lifetimes measured in  $H_2O$  and  $D_2O$ , Soderholm et al. concluded that the two sites were not simultaneously occupied in the same anion, and that the Eu was coordinated to three water molecules in site A and to two water molecules in site B. Furthermore, the  $^{31}P$  NMR chemical shift for the europium derivative in 1 M HCl reported by Soderholm et al. was significantly different from that reported earlier for less acidic solutions of the derivative and this observation raises questions about the solution behavior of Preyssler anion derivatives in general. We have since reported the structures of salts  $(K_{0.5}(NH_4)_{11.5}[EuP_5W_{30}O_{110}] \cdot 24H_2O)$  (**Eu**) and  $K_6H_6[EuP_5W_{30}O_{110}] \cdot 31H_2O$  (**HEu**) of the europium derivative isolated from neutral and acid solutions, respectively, and of the uranium derivative isolated from neutral solution  $((NH_4)_{11}[UP_5W_{30}O_{110}] \cdot 12H_2O)$  (**U**).<sup>6</sup> These structures revealed no significant differences between the environments of the

(5) Soderholm L.; Liu, G. K.; Munteau, J.; Malinsky, J.; Antonio, M. R. *J. Phys. Chem.* **1995**, *99*, 9611.

(6) Dickman, M. H.; Gama, G. J.; Kim, K.-C.; Pope, M. T. *J. Cluster Sci.* **1996**, *7*, 567.

**Table 1.** Analytical Data<sup>a</sup> for X<sub>n</sub>[M(OH<sub>2</sub>)P<sub>5</sub>W<sub>30</sub>O<sub>110</sub>](y - 1)H<sub>2</sub>O

compd	X <sub>n</sub>	M	P	W	H <sub>2</sub> O (y)
<b>Ca</b>	(NH <sub>4</sub> ) <sub>13</sub>	Ca			
	N: 2.25(2.18)	0.35(0.48)	1.75(1.86)	66.20(66.17)	35
<b>HCa</b>	K <sub>6</sub> H <sub>7</sub>	Ca			
	K: 2.82(2.75)	0.38(0.47)	1.68(1.82)	64.60(64.71)	45
<b>Y</b>	(NH <sub>4</sub> ) <sub>12</sub>	Y			
	N: 2.36(2.03)	1.44(1.07)	1.73(1.87)	65.04(66.64)	30
<b>HY</b>	K <sub>6</sub> H <sub>6</sub>	Y			
	K: 2.79(2.77)	1.37(1.05)	1.74(1.83)	65.09(65.04)	40
<b>HU</b>	K <sub>6</sub> H <sub>6</sub>	U			
	K: 2.84(2.75)	1.85(1.77)		63.56(64.53)	41
	H: 0.84(1.03)				

<sup>a</sup> Calculated values in parentheses.

europium ion (1.763 and 1.760 Å, respectively, from the equatorial plane of the anion defined by the phosphorus atoms) that could account for the observations of Soderholm et al. There were, however, two unexpected features of these structures: the presence of an “internal” water molecule coordinated to the encrypted cation, and a significant displacement of the Eu<sup>3+</sup> and U<sup>4+</sup> cation positions, compared with that previously reported for the sodium derivative, toward the exterior of the anion.

We have therefore examined the structures of cation derivatives with other charges (Ca<sup>2+</sup>, Y<sup>3+</sup>) and have reexamined the structure of the sodium derivative at low temperature. In every case the internal cation is axially solvated by a single water molecule that is nonlabile on the NMR time scale. The position of the cation on the anion's C<sub>5</sub> axis is influenced by cation charge and radius, and in some cases by protonation of the anion. Careful examination of the pH and time dependence of <sup>1</sup>H and <sup>31</sup>P NMR spectra of the paramagnetic europium derivative demonstrates unique acid–base behavior for an aqueous system. Protonation occurs at a relatively inaccessible oxygen site on the “internal” surface of the heteropolyanion, resulting in slow proton exchange with solvent water.

We also present evidence that a “metal-free” anion is formed under very acidic conditions.

## Experimental Section

**Syntheses.** Potassium salts of the calcium, yttrium, and lanthanide derivatives were prepared by a slight modification of the published method.<sup>4</sup> Two equivalents of the metal ion (nitrate) and 1 equiv of the potassium salt of the Preyssler anion were dissolved in water and the hydrothermal reactions were carried out at 170 °C for 3 days. For the uranium derivative, 5 equiv of UCl<sub>4</sub> dissolved in water was added to 1 equiv of the Preyssler anion dissolved in water, and the reaction was carried out at 170 °C for 4 days. The reactions were followed by precipitation of the products by adding solid KCl to the reaction media. The products were identified by <sup>31</sup>P NMR spectroscopy and cyclic voltammetry.

Crystals suitable for single-crystal X-ray analysis were grown as follows. For crystals of the ammonium salts, saturated NH<sub>4</sub>Cl was added dropwise to an aqueous solution of the potassium salt, and solvent was allowed to evaporate at room temperature. For the ammonium salt of the calcium derivative, the crystals were grown at pH 8 adjusted by adding a few drops of 18 M ammonia to an aqueous solution of the potassium salt. The protonated and unprotonated species of the calcium derivative coexist between pH 4 and 6 according to <sup>31</sup>P NMR.

Crystals of the acid salts were grown by dissolving the potassium salts in 4 M HCl and allowing the solvent to evaporate in a desiccator over concentrated sulfuric acid. To prevent loss of HCl from the solution during the crystallization, the atmosphere in the desiccator was enriched with HCl(g) by adding a small amount of KCl to the H<sub>2</sub>SO<sub>4</sub> reservoir. Analytical data for the crystals examined are summarized in Table 1.

**Crystallography.** Crystals were examined under a thin layer of mineral oil using a polarizing microscope. Selected crystals were mounted on a glass fiber and quickly placed in a stream of cold nitrogen

on a Siemens SMART CCD diffractometer for the structures of **Na** (ammonium salt of the Preyssler anion), **Ca** (ammonium salt of the calcium derivative), **HCa** (potassium acid salt of the calcium derivative), **Y** (ammonium salt of the yttrium derivative), **HY** (potassium acid salt of the yttrium derivative), and **HU** (potassium acid salt of the uranium derivative). All data collection was performed at 173(2) K. The structures were solved by direct methods locating the heaviest atoms, and the remaining atoms were found in subsequent Fourier difference syntheses. In **Na** and **Y**, occupancy factors were varied in early stages of refinement for the two chemically equivalent metal ion sites. In the final refinement, the factors were rounded off and held fixed. All atoms except oxygen atoms and disordered cations were refined anisotropically. Nitrogen atoms of ammonium cations for **Na**, **Ca**, and **Y** were modeled as oxygen atoms because nitrogen atoms could not be distinguished from oxygen atoms. No hydrogen atoms were included in the models. All refinements were full-matrix least squares on *F*<sup>2</sup>. Crystal data and structure refinement parameters are listed in Table 2. Final atomic coordinates and displacement parameters of the structures are given in the Supporting Information. Selected bond distances in the five structures are given in Table 3.

**NMR Spectroscopy.** All NMR spectra were recorded using a Bruker AM-300WB spectrometer operating at 7.05 T (300.13 MHz for proton). The resonance frequencies are 121.495 MHz for <sup>31</sup>P and 12.483 MHz for <sup>183</sup>W. Chemical shifts are given with respect to TMS for proton, external 85% H<sub>3</sub>PO<sub>4</sub> for <sup>31</sup>P, and 2 M Na<sub>2</sub>WO<sub>4</sub> for <sup>183</sup>W. Downfield shifts are recorded as positive.

**Hydrothermal Treatment.** The potassium salt of **Na** was dissolved at pH 2.0 (sulfate buffer) and in 0.1, 1, 2, 4, and 6 M HCl. The solutions sealed in Teflon-lined Parr acid digestion bombs were heated at 170 °C for 24 h.

**Sodium Activity Measurement.** Sodium ion activities were measured with a sodium electrode (Orion Model 94-11). All such measurements were made in an ammonium buffer (20 g of NH<sub>4</sub>Cl and 5 mL of 18 M NH<sub>3</sub> in 100 mL, pH 8.5) contained in a Teflon beaker. The electrode response was found to be linear up to [Na<sup>+</sup>] = 0.01 M. All the solutions for measurement of sodium ion activity were prepared with water purified by a Milli-Q Plus system (18 MΩ·cm). All unknown concentrations were determined by a standard curve method with repeat measurements.

K<sub>12.5</sub>Na<sub>1.5</sub>[NaP<sub>5</sub>W<sub>30</sub>O<sub>110</sub>]·15H<sub>2</sub>O was converted to the free acid using H<sup>+</sup>-form Dowex-50 ion-exchange resin before hydrothermal treatment in acidic solutions. H<sub>14</sub>[NaP<sub>5</sub>W<sub>30</sub>O<sub>110</sub>] (1.00 g, 0.13 mmol) was dissolved in 10 mL of 2 M HCl, and the sodium ion activity was measured in a Teflon container. The solution was heated at 170 °C for 24 h, and the sodium ion activity was measured again.

## Results and Discussion

**Structures. (a) Internal Water Molecule.** The main features of the structures of the heteropolyanions are as previously reported,<sup>3,6</sup> see Figures 1 and 2. The water molecule coordinated to the internal cation observed in the structures of the europium and uranium derivatives is confirmed for all the structures reported here, including that of the sodium derivative, **Na**.

As originally described,<sup>3</sup> the anion has two possible metal coordination sites. One, S<sub>1</sub>, is in the very middle of the anion, formed by 10 phosphate oxygens; the other site, S<sub>2</sub>, is formed by five phosphate oxygens and five oxygens which bridge two tungsten atoms each. There are two equivalent S<sub>2</sub> sites per anion. In both the previous and current structures of **Na**, the Na<sup>+</sup> ion occupies a position near an S<sub>2</sub> site, but is displaced toward the center of the anion. As a result of crystallographic disorder the sodium ion appears to be distributed equally between this site and an equivalent site in the other half of the anion. Regardless of the site occupied, there is insufficient room in the anion for both sites to be simultaneously occupied by a cation.

A water molecule coordinated to the sodium ion was not reported in the previous structure of anion **Na**.<sup>3</sup> This almost certainly results from the poorer resolution of a limited data

**Table 2.** Crystal and Refinement Parameters

	Na	Ca	HCa	Y	HY	HU
formula	(NH <sub>4</sub> ) <sub>14</sub> NaP <sub>5</sub> W <sub>30</sub> O <sub>110</sub> · 28H <sub>2</sub> O	(NH <sub>4</sub> ) <sub>13</sub> CaP <sub>5</sub> W <sub>30</sub> O <sub>110</sub> · 24H <sub>2</sub> O	K <sub>5</sub> H <sub>8</sub> CaP <sub>5</sub> W <sub>30</sub> O <sub>110</sub> · 43H <sub>2</sub> O	(NH <sub>4</sub> ) <sub>12</sub> YP <sub>5</sub> W <sub>30</sub> O <sub>110</sub> · 24H <sub>2</sub> O	K <sub>5</sub> H <sub>7</sub> YP <sub>5</sub> W <sub>30</sub> O <sub>110</sub> · 31H <sub>2</sub> O	K <sub>3</sub> H <sub>8</sub> UP <sub>5</sub> W <sub>30</sub> O <sub>110</sub> · 21H <sub>2</sub> O
FW	8210.6	8137.6	8448.9	8168.3	8280.4	8172.2
cryst syst	triclinic	monoclinic	monoclinic	monoclinic	monoclinic	monoclinic
space group	<i>P</i> $\bar{1}$	<i>P</i> 2 <sub>1</sub> / <i>m</i>	<i>P</i> 2 <sub>1</sub> / <i>m</i>	<i>P</i> 2 <sub>1</sub> / <i>c</i>	<i>C</i> 2/ <i>c</i>	<i>P</i> 2 <sub>1</sub> / <i>m</i>
temp (K)	173(2)	173(2)	173(2)	173(2)	173(2)	173(2)
color	colorless	colorless	colorless	colorless	colorless	brown
<i>a</i> (Å)	17.464(4)	17.7526(3)	17.4987(2)	17.52550(10)	17.6012(8)	16.9079(6), 16.9079(6),
<i>b</i> (Å)	17.766(3)	21.1054(4)	21.5054(3)	21.0554(2)	28.1222(13)	20.9969(7), 20.9969(7),
<i>c</i> (Å)	23.510(3)	17.8629(2)	17.54970(10)	35.5201(2)	24.6158(11)	17.8737(6)
$\alpha$ (deg)	97.351(11)					
$\beta$ (deg)	98.298(8)	104.5050(10)	104.8080(10)	104.1420(10)	109.3110(10)	113.7860(10)
$\gamma$ (deg)	112.13(2)					
Z	2	2	2	4	4	2
GOF	1.102	1.060	1.029	1.065	1.267	1.119
<i>R</i> [ <i>I</i> > 2 $\sigma$ ( <i>I</i> )]	<i>R</i> 1 = 0.0560, <i>wR</i> 2 = 0.1230	<i>R</i> 1 = 0.0836, <i>wR</i> 2 = 0.2176	<i>R</i> 1 = 0.0585, <i>wR</i> 2 = 0.1456	<i>R</i> 1 = 0.0623, <i>wR</i> 2 = 0.1438	<i>R</i> 1 = 0.0835, <i>wR</i> 2 = 0.1734	<i>R</i> 1 = 0.0699, <i>wR</i> 2 = 0.1582

**Table 3.** Selected Average Bond Distances<sup>a</sup> (Å)

	Na	Ca	Y	HCa	HY	HU
W–O( <i>b</i> ) <sup>b</sup> (short)						
range	1.80(2)–1.85(2)	1.91(2)–1.97(2)	1.87(2)–1.98(2)	1.85(2)–1.89(2)	1.87(2)–1.91(2)	1.91(2)–1.98(2)
mean	1.82[2]	1.94[2]	1.93[3]	1.87[1]	1.90[1]	1.94[2]
W–O( <i>b</i> ) <sup>b</sup> (long)						
range	2.02(2)–2.09(2)			1.95(2)–2.01(2)	1.93(2)–1.99(2)	
mean	2.06[2]			1.99[2]	1.96[2]	
W–O1,2,3P <sup>c</sup>						
range	2.22(2)–2.31(2)	2.24(2)–2.28(2)	2.23(2)–2.30(2)	2.25(2)–2.30(2)	2.23(2)–2.33(2)	2.29(2)–2.38(2)
mean	2.27[2]	2.26[2]	2.26[2]	2.27[1]	2.28[3]	2.32[3]
W–O4P <sup>d</sup>						
range	2.18(2)–2.21(2)	2.20(2)–2.23(2)	2.14(2)–2.18(2)	2.22(2)–2.26(2)	2.20(2)–2.33(2)	2.27(2)–2.41(2)
mean	2.20[1]	2.21[2]	2.16[1]	2.24[1]	2.26[4]	2.32[5]
M–O1M	2.32(4)	2.25(3)	2.16(2)	2.35(3)	2.28(3)	2.33(3)
M–O( <i>e</i> )						
range	2.95(2)–3.01(2)	2.88(2)–2.92(2)	2.66(2)–2.83(2)	2.87(2)–2.94(2)	2.68(2)–2.92(2)	2.630(14)–2.727(18)
mean	2.99[2]	2.90[1]	2.73[5]	2.89[3]	2.78[11]	2.67[4]
M–O(P)						
range	2.61(2)–2.69(2)	2.63(2)–2.72(2)	2.53(2)–2.67(2)	2.60(2)–2.64(2)	2.54(2)–2.68(2)	2.626(14)–2.700(15)
mean	2.64[3]	2.68[3]	2.60[5]	2.62[1]	2.61[5]	2.66[3]
O1M–O(P)						
range	2.63(4)–2.70(3)	2.70(4)–2.78(4)	2.74(2)–2.82(2)	2.63(3)–2.66(3)	2.64(4)–2.70(4)	2.66(3)–2.82(3)
mean	2.67[2]	2.73[4]	2.78[3]	2.65[1]	2.67[2]	2.73[7]

<sup>a</sup> Parentheses indicate estimated standard deviations; square brackets indicate calculated standard deviations. M indicates Na, Ca, Y, or U as appropriate. <sup>b</sup> All W–O(*b*) bond lengths for Ca, Y, and HU are included in this category. <sup>c</sup> The values for Na and Ca include only W–O2P and W–O3P bond lengths. <sup>d</sup> The values for Na and HY include W–O1P and W–O4P bond lengths, and the values for Ca are W–O1P bond lengths.

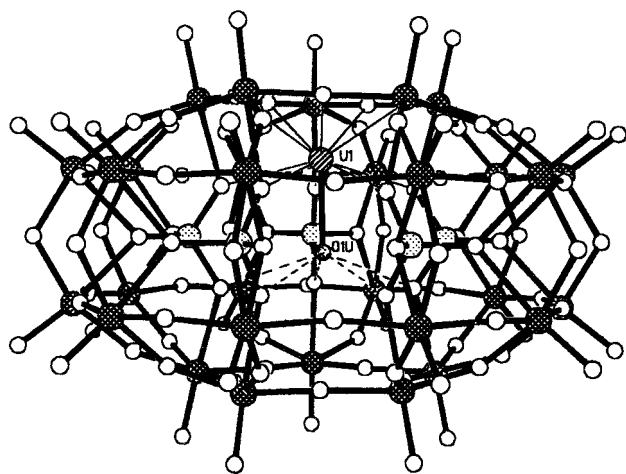


**Figure 1.** Ball-and-stick representation of the structure of anion HU (side view) showing the position of the uranium cation and its associated water molecule. Probable hydrogen bond interactions are indicated by broken lines.

set ( $\theta_{\max} = 18^\circ$ ) collected at room temperature in that work. Resolution of atom positions depends on the maximum  $\theta$  angle as well as on thermal vibrations. In the present study, using data collected to  $\theta_{\max} = 28.37^\circ$  at 173 K, the water molecule

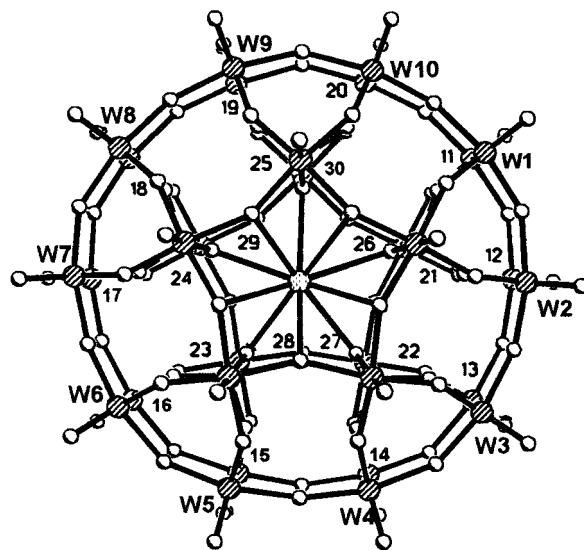


**Figure 2.** Ball-and-stick representation of the structure of anion HU (top view) showing numbering of tungsten atoms.

bound to the sodium ion could just be resolved. The distances between the peaks corresponding to the sodium cation (Na1) and the water molecule coordinated to the “other”, disordered,

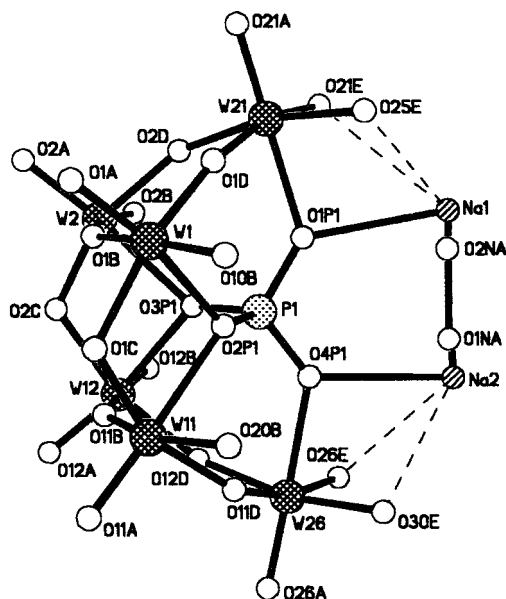


**Figure 3.** Side view of a portion of the structure of the sodium derivative **Na** showing the two sites of the disordered internal cation and water molecule.

**Table 4.** Relative Position of the Internal Cation in  $[M(H_2O)P_5W_{30}O_{110}]^{n-}$

cation	distance from equatorial plane (Å)		radius <sup>a</sup>
	ammonium salt	acid salt	
Na <sup>+</sup>	1.552		1.38
Ca <sup>2+</sup>	1.650	1.641	1.32
Eu <sup>3+</sup>	1.763 <sup>b</sup>	1.760 <sup>b</sup>	1.26
Y <sup>3+</sup>	1.747	1.794	1.215
U <sup>4+</sup>	1.931 <sup>b</sup>	1.998	1.19

<sup>a</sup> For 9-fold coordination [Shannon, R. D. *Acta Crystallogr.* **1976**, A32, 751]. <sup>b</sup> Reference 6.

cation (O2Na), and between the corresponding pair, Na2 and O1Na, are 0.69(3) and 0.72(3) Å, respectively (see Figure 3). These distances are at about the limit for data collected to  $\theta = 28.37^\circ$  but could not be resolved with the earlier less-complete data set. Consequently the sodium cation position reported earlier was taken from the average position of the overlapping (Na + O) peaks at 1.25 Å from the equatorial plane. With the higher resolution afforded by the present study, the sodium position can be corrected to 1.52(3) Å from the equator.

**(b) Position of Internal Cation.** As indicated in the structures of the europium and uranium derivatives reported earlier, the positions of the internal cations differed significantly. Table 4 summarizes the results of all structural determinations.

The following comments may be made about these data. First, there is an obvious effect of cation charge; the more highly charged cations are found closer to the center of the pentagonal antiprism formed by five phosphate oxygens and five oxygens that bridge two tungstens ( $S_2$  site), and this equalizes the electrostatic interactions with the 10 oxygens. As shown by the data in Table 3, the mean values of the M–O(W<sub>2</sub>) bonds decrease from 2.99 to 2.59 Å as M changes from Na to U, whereas the mean values of M–O(P) remain almost unchanged (range 2.60–2.65 Å). An alternative rationalization of the cation position might be made on the basis of ionic radius, but this is a quantitatively less well-defined parameter than charge. The coordination number of the internal cation is 11 (monocapped pentagonal antiprism), but comparable literature values are only available for 9-coordination. Second, for the smallest cations (Y<sup>3+</sup>, U<sup>4+</sup>) there are significant differences between protonated

and unprotonated anions that probably reflect the effects of the internal protonation (see below)

**Crystallographic Disorder.** Crystal structures of polyoxometalates can often show orientational disorder of the anion, site disorder of the counterions and water, or both. The disorder of heteropolyanions can generally be attributed to their high symmetry, which allows them to assume two or more orientations at one crystallographic site. Disorder of the cations or loosely bound water usually takes the form of fractional occupancy among several sites. Both types of disorder are seen in the structures studied here.

The encrypted metal cation was found to be equally disordered over equivalent sites on both sides of the anion in **Na** and is required to be so disordered as a result of a crystallographic mirror plane in the structures of **Ca**, **HCa**, and **HU** and as a result of a crystallographic 2-fold axis in the structure of **HY**. In **Y**, the metal ions are not equally disordered at the two equivalent sites. The Y<sup>3+</sup> cation in **Y** is disordered approximately 75/25%. Similar disorders were noted earlier for the Eu<sup>3+</sup> (70/30%) and U<sup>4+</sup> (75/25%) derivatives.<sup>6</sup> The asymmetry of the anion induced by the partial disorder of the central metal ion in **Y** and in the ammonium salts of the europium and uranium derivatives<sup>6</sup> is also reflected in the tungsten–oxygen distances to the phosphate oxygens in the lower part of the anion (W–O4P<sub>n</sub>) compared with the other phosphate oxygens (W–O1, 2, 3P<sub>n</sub>), see Table 3.

The salts exhibiting partial ordering of the anions are those in which the central cation (Y, Eu, U) is most strongly displaced from the equator of the anion, suggesting that the ordering results from weak dipole–dipole forces. That none of the acid salts shows preferential ordering would be consistent with the idea that anion protonation results in (partial) cancellation of the anion's polarity.

The bond distances between the encrypted metal ion and the water oxygen atom fall in the range 2.16(2)–2.35(3) Å. Although these distances cannot be measured to high precision, in every case the bond lengths in the acid salts appear to be somewhat larger (by an average of 0.13 Å) than in the corresponding normal salts. Such a variation is considered to be statistically significant ( $\Delta \geq 3\sigma$  in three out of four cases), and would be consistent with the internal protonation discussed below.

**NMR Spectroscopy.** Our earlier paper had reported the <sup>31</sup>P chemical shifts (*A*) for several derivatives of the Preyßler anion measured in neutral or weakly acidic solution. Following the subsequent report of a very different chemical shift (*B*) for the europium derivative in strongly acidic media, we have reexamined several other derivatives in both acidic and neutral solutions. The results are summarized in Table 5.

The magnitudes of some of these pH-dependent shifts are not unprecedented for paramagnetic species. We have observed a 200-ppm change for  $\delta(^{31}\text{P})$  between  $[\text{PW}_{11}\text{O}_{39}\text{Ru}(\text{OH}_2)]^{4-}$  and  $[\text{PW}_{11}\text{O}_{39}\text{Ru}(\text{OH})]^{5-}$ , for example.<sup>7</sup> However, the chemical shift changes illustrated in Table 5 are not continuous. In solutions of intermediate acidity *both A and B peaks are observed, unbroadened, with relative intensities that correlate with solution pH*. This implies that proton exchange between protonated (peak B) and unprotonated (peak A) anions is slow

(7) Rong, C.; Pope, M. T. *J. Am. Chem. Soc.* **1992**, *114*, 2932–2938.

(8) (a) Kristjánssdóttir, S. S.; Norton, J. R. In *Transition Metal Hydrides: Recent Advances in Theory and Experiment*; Dedieu, A., Ed.; VCH: New York, 1992; pp 309–359. (b) Kramarz, K. W.; Norton, J. R. *Prog. Inorg. Chem.* **1994**, *42*, 1–65. (c) La, T.; Miskelly, G. M. *J. Am. Chem. Soc.* **1995**, *117*, 3613. (d) Liu, W.; Thorp, H. H. *J. Am. Chem. Soc.* **1995**, *117*, 9822.

**Table 5.**  $\delta(\text{P})/\text{ppm}$  for  $\text{MP}_5\text{W}_{30}$  at pH 4 (A) and in 2 M HCl (B)

M	A	B	$\Delta(A - B)$	M	A	B	$\Delta(A - B)$
Ca(II)	-9.0 <sup>a</sup>	-11.1 <sup>b</sup>	2.1	Eu(III)	0.6	-9.1	9.7
Y(III)	-10.2	-9.0	-1.2	Tb(III)	-27.2	24.1	-51.3
Ce(III)	-16.1	-10.5	-5.6	Tm(III)	17.0	-9.9	26.9
Nd(III)	-21.6	-12.5	-9.1	U(IV) <sup>c</sup>	-75.9	-76.2	0.3
Sm(III)	-9.6	-7.4	-2.2				

<sup>a</sup> pH 8. <sup>b</sup> pH 1. <sup>c</sup> The <sup>31</sup>P NMR chemical shift of the U<sup>4+</sup> derivative was originally reported at -15.5 ppm. (ref 4a), but we have been unable to reproduce this. The present value and the small effect of protonation can be attributed to a dominant contact (scalar) contribution to the isotropic shift in the case of U compared with the lanthanides.

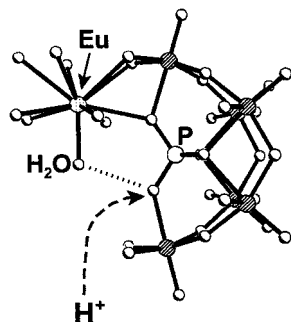


**Figure 4.** One-fifth of the tungstophosphate framework of the europium derivative of the Preyssler anion showing the coordination environment of the Eu<sup>3+</sup> cation and its axial aqua ligand. One of the five equivalent possible "internal" protonation sites is shown. The dotted line indicates a probable hydrogen bond interaction.

on the NMR time scale ( $k_{\text{eff}} \ll 10^{-3} \text{ M}^{-1} \text{ s}^{-1}$  for the Eu<sup>3+</sup> derivative). Despite considerable current interest in slow proton-transfer reactions,<sup>8</sup> we can discover no precedent for such a slow rate between oxygen centers in aqueous solution.<sup>9-11</sup> We therefore conclude that the rate is controlled by steric factors,<sup>12</sup> and that the exchanging proton is located *inside the central cylindrical cavity of the anion*. The cavity is lined by 10 phosphate oxygen atoms which are arguably the most basic (negative) sites on the internal surface of the empty (metal-free) heteropolyanion. The charges borne by five of these oxygens are partly compensated by the charge of the encrypted metal cation. The second set of five oxygens are at an appropriate distance, 2.66–2.78 Å (Table 3), to participate in H-bonding with the protons of the internal water molecule, which is presumed to undergo free rotation. We postulate that when *one* of these oxygen atoms is protonated (as shown in Figure 4) the P NMR spectrum exhibits the chemical shift of line B (Table 5). Since only a single NMR line is observed, intramolecular proton exchange among the five equivalent oxygens must be rapid (but see below for further discussion).

(9) Although proton transfer to and from transition metals involves electronic barriers that can result in rate constants as low as  $10^{-3} \text{ M}^{-1} \text{ s}^{-1}$ , proton transfer to oxo, hydroxo, and aquo ligands is considerably faster ( $10^4$ – $10^{11} \text{ M}^{-1} \text{ s}^{-1}$ ) even when determined in acetonitrile solution, see ref 8b.

(10) Proton transfer between highly charged polyoxometalate anions in acetonitrile and similar nonaqueous solvents is frequently slow on NMR and voltammetric time scales, see, for example: Finke, R. G.; Rapko, B.; Saxton, R. J.; Domaille, P. J. *J. Am. Chem. Soc.* **1986**, *108*, 1986. Harmalkar, S. P.; Pope, M. T. *J. Inorg. Biochem.* **1986**, *28*, 85.

(11) Slow irreversible proton transfer converting metastable  $[\text{HW}_{12}\text{O}_{40}]^{7-}$ , which has a single proton in the central tetrahedral cavity of the Keggin structure, into metatungstate anion,  $[\text{H}_2\text{W}_{12}\text{O}_{40}]^{6-}$ , with two central protons, has been observed and measured in aqueous solution [Launay, J. P. *J. Inorg. Nucl. Chem.* **1976**, *38*, 807]. The singly protonated anion *cannot* be prepared by partial neutralization of metatungstate.

(12) Steric effects have been invoked to account for abnormally low rates of deprotonation of transition metal hydrides, e.g.  $[\text{H}_4\text{Re}(\text{PMe}_2\text{Ph})_4]^+$  and  $[\text{HMo}(\text{CO})_2(\text{dppe})_2]^+$  [Kristjánssdóttir, S. S.; Loendorf, A. J.; Norton, J. R. *Inorg. Chem.* **1991**, *30*, 4470. Darensbourg, M. Y.; Ludvig, M. M. *Inorg. Chem.* **1986**, *25*, 2894].

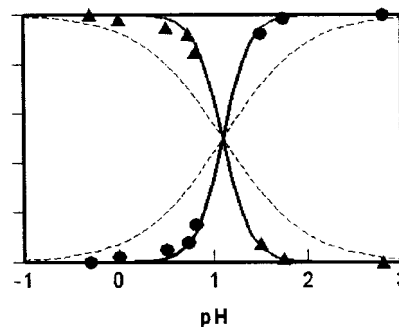
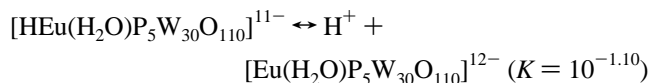


**Figure 5.** Relative intensities of the <sup>31</sup>P NMR signals of  $[\text{Eu}(\text{H}_2\text{O})\text{P}_5\text{W}_{30}\text{O}_{110}]^{12-}$  as a function of solution pH. Triangles,  $\delta = -9.1$ ; circles,  $\delta = +0.6$  ppm. Solid lines were computed as described in the text for the model in which  $\text{p}K_1(\text{ext}) + \text{p}K_2(\text{ext}) + \text{p}K_3(\text{int}) = 3.30$ . Broken lines are computed for the model in which  $\text{p}K(\text{int}) = 1.10$ .

We have chosen to examine the europium derivative in more detail, since the NMR lines are narrow (ca. 10 Hz) and the chemical shift change is large. Spectra were recorded on freshly prepared solutions (see below) of the potassium salt in 2 M HCl (pH “-0.3”), 1 M HCl (pH 0), and sulfate, citrate, and acetate buffers, the pH of which was adjusted by addition of small amounts of HCl and NaOH. The relative intensities of the 0.6- and -9.1-ppm lines were measured for each solution. The results could be reproduced when the final pH was approached from either direction. As shown in Figure 5 the transition from a solution in which the “protonated” species was dominant occurred over a narrow range of pH in a strongly acidic regime (apparent “pK” = 1.10). The rather abrupt change from spectrum B to spectrum A cannot be modeled assuming the single protonation equilibrium,



(see broken lines in Figure 5). However, a satisfactory fit of the data can be made if it is assumed that at pH 0 the anion is “internally” protonated (by one proton) and “externally” protonated (by *at least two* protons),  $(\text{H}_{\text{ext}})_n(\text{H}_{\text{int}})\text{EuP}_5\text{W}_{30}\text{O}_{110}]^{(11-n)-}$ , and that only removal of the “internal” proton affects the phosphorus chemical shift. There are many plausible external protonation sites (e.g. oxygen atoms shared by two tungstens), analogous to those on the surfaces of Keggin anions, for example. The solid lines in Figure 5 are calculated assuming (1) that *two* of the external protons are removed *before* the internal proton, (2) that  $\text{p}K_{a1}(\text{ext}) + \text{p}K_{a2}(\text{ext}) + \text{p}K_{a3}(\text{int}) = 3(1.10)$ , and (3) that the intensity of the -9.1-ppm signal (B) measures the sum of the concentrations of all species containing the internal proton, and that of the 0.6-ppm signal (A) measures the sum of the concentrations of all species that lack the internal proton. It is not possible with the present data to determine whether any external protons remain bound to the anion at pH > 2 (or in other words if there are more than two bound external protons under acidic conditions, pH ~0). Analogous calculations assuming prior removal of one or three external protons give marginally worse fits to the experimental data than the one shown.

Whether the internal proton  $\text{H}_{\text{int}}$  is considered to be bonded to a phosphate oxygen (and hydrogen-bonded to the internal water molecule) as represented in Figure 4 or whether the water molecule itself is protonated to form a hydronium ion (hydrogen bonded to the phosphate oxygens) is difficult if not impossible to establish. Certainly, within the cavity, hydrogen bonds are

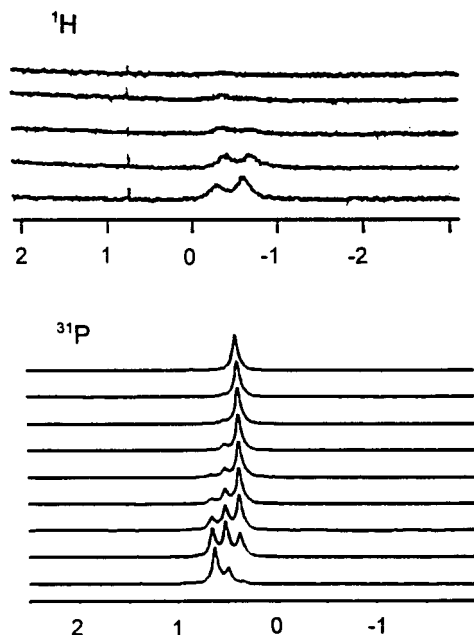


**Figure 6.** Time-dependence of  $^1\text{H}$  and  $^{31}\text{P}$  NMR spectra of  $[\text{Eu}(\text{H}_2\text{O})\text{P}_5\text{W}_{30}\text{O}_{110}]^{12-}$  in  $\text{D}_2\text{O}$ , pD 3.6, ca. 28 °C. Traces from bottom to top: ( $^1\text{H}$ ) 10, 40, 100, and 160 min, 14 h; ( $^{31}\text{P}$ ) 10, 40, 70, 100, 130, 160, 140, and 280 min, 18 h.

rapidly being formed, broken, and reformed to maintain NMR equivalence of the five phosphorus nuclei.<sup>13</sup> Even if, as seems most likely, the ground state can be represented by  $\text{P}-\text{O}-\text{H}_{\text{int}} \cdot \cdot \text{OH}_2(\text{Eu})$ , the barrier to H-bond reorganization leading to exchange of  $\text{H}_{\text{int}}$  with a proton of the internal water molecule would be very low. The apparent increase in  $\text{M}-\text{OH}_2$  bond distance noted above for the protonated anions is understandable in terms of either possible tautomer,  $\text{HO}(\text{P})$  or  $\text{H}_3\text{O}(\text{Eu})$ .

**Time Dependence of NMR Spectra.** Although freshly prepared solutions of the potassium salts of the europium and uranium derivatives give a single P NMR peak in neutral or weakly acidic solutions, aged solutions often showed a splitting of the peaks. This was originally assumed to indicate a slow process involving a reduction in the symmetry of the heteropolyanion, but with the recognition that the anions contained an internal water molecule, the possibility of H/D exchange on the water molecule resulting in isotopomer formation could be considered. This has proved to be the explanation for the time dependence of the NMR spectra. Figure 6 shows the  $^1\text{H}$  and  $^{31}\text{P}$  NMR spectra of a solution of the potassium salt of the europium derivative dissolved in 100%  $\text{D}_2\text{O}$  (pD = 3.6). The proton spectrum shows two lines, at  $-0.32$  and  $-0.63$  ppm, which slowly decrease in intensity. These are attributed to the isotopomers with internal  $\text{H}_2\text{O}$  and HDO molecules. Since the peak at  $-0.63$  vanishes more rapidly it is assigned to the anion incorporating  $\text{H}_2\text{O}$ . As expected, the phosphorus spectra show as many as three peaks at 0.64, 0.51, and 0.37 ppm (corresponding to  $\text{H}_2\text{O}$ , HDO, and  $\text{D}_2\text{O}$  isotopomers, respectively), the intensities of which follow a precedented pattern (Table S2 in Supporting Information, and Figure 7) corresponding to the consecutive pseudo-first-order exchange reactions

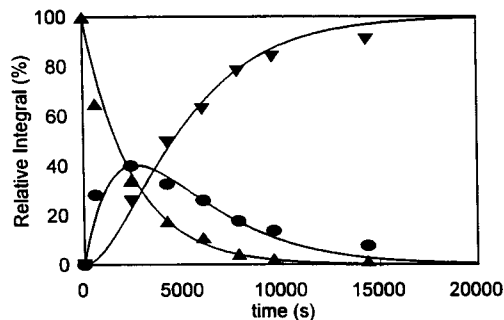


**Figure 7.** Relative integrated intensities of  $^{31}\text{P}$  NMR lines at 0.64, 0.51, and 0.37 ppm corresponding to  $\text{H}_2\text{O}$ , HDO, and  $\text{D}_2\text{O}$  isotopomers respectively of  $[\text{Eu}(\text{H}_2\text{O})\text{P}_5\text{W}_{30}\text{O}_{110}]^{12-}$  as a function of time. Conditions as for Figure 6. Solid lines are computed from the equations given in the text for  $k_1 = 4.1 \times 10^{-4}$  and  $k_2 = 3.4 \times 10^{-4} \text{ s}^{-1}$ .



Values of  $k_1$  ( $4.1(2) \times 10^{-4} \text{ s}^{-1}$ ) and  $k_2$  ( $3.4(2) \times 10^{-4} \text{ s}^{-1}$ ) were obtained from a nonlinear Simplex fit, shown as the solid lines in Figure 7, of the experimental data to the equations

$$[\text{A}]_t = [\text{A}]_0 e^{-k_1 t}$$

$$[\text{B}]_t = k_1 [\text{A}]_0 \frac{e^{-k_1 t} - e^{-k_2 t}}{k_2 - k_1}$$

$$[\text{C}]_t = [\text{A}]_0 \left( 1 + \frac{k_1 e^{-k_2 t} - k_2 e^{-k_1 t}}{k_2 - k_1} \right)$$

where  $\text{A} = \text{H}_2\text{O}$ ,  $\text{B} = \text{HDO}$ , and  $\text{C} = \text{D}_2\text{O}$

Preliminary qualitative experiments show that the effective rate of H/D exchange is highly dependent upon solution acidity: development of the split spectrum was noticeably slower at pH 5. At pH 7.5 the line remained unsplit after two months. These observations indicate that exchange can only occur when the anion is internally protonated. Further investigation is in progress.

Resolution of the H/D isotopomers can be observed in the P NMR spectra of other paramagnetic derivatives ( $\text{Ce}^{3+}$ ,  $\text{Nd}^{3+}$ ,  $\text{U}^{4+}$ ) but not for the  $\text{Tb}^{3+}$  and  $\text{Tm}^{3+}$  derivatives because of broad lines, and not for the diamagnetic anions ( $\text{Ca}^{2+}$  and  $\text{Y}^{3+}$ ).

**Evidence for a Metal-Free Heteropolyanion.** When hydrothermal exchange reactions of **Na** with other metal cations were carried out in strongly acidic solutions (pH < 1) a P NMR signal was observed at  $-9.8$  ppm (in addition to that of **Na** at  $-9.5$  ppm, and in addition to lines attributable to the other metal-substituted species). Hydrothermal treatment of solutions containing only **Na** showed that the  $-9.8$ -ppm peak gained in intensity as the acidity was increased, Figure 8. A tungsten NMR spectrum that was recorded on a solution treated in 2 M HCl showed five lines at  $-209.6$ ,  $-211.7$ ,  $-277.4$ ,  $-287.8$ , and  $-289.8$  ppm (Figure 8b). This spectrum can be decomposed into the four-line spectrum of **Na**,  $-209.6(1\text{W})$ ,  $-211.7(1\text{W})$ ,  $-277.4(2\text{W})$ , and  $-289.8(2\text{W})$ , and a two-line spectrum of a new complex,  $-211.7(1\text{W})$  and  $-287.8(2\text{W})$ . The similarity of the chemical shifts strongly suggests that the new complex is still a  $\text{P}_5\text{W}_{30}$  anion, but with  $D_{5h}$  symmetry rather than  $C_{5v}$ . Such a symmetry change could be the result of the sodium cation moving into the equatorial plane of the anion, or to loss of the sodium entirely. Measurement of sodium ion activities before and after hydrothermal treatment demonstrates that the second explanation is correct. A sample of 1.00 g of the free acid of

(13) The disposition and time-dependence of hydrogen bonds within the central tetrahedral cavity of the metatungstate anion  $[\text{H}_2\text{W}_{12}\text{O}_{40}]^{6-}$  and analogous F-substituted derivatives (see, for example: Chauveau, F.; Doppelt, P.; Lefebvre, J. *Inorg. Chem.*, **1980**, *19*, 2803) presents a similar conundrum.

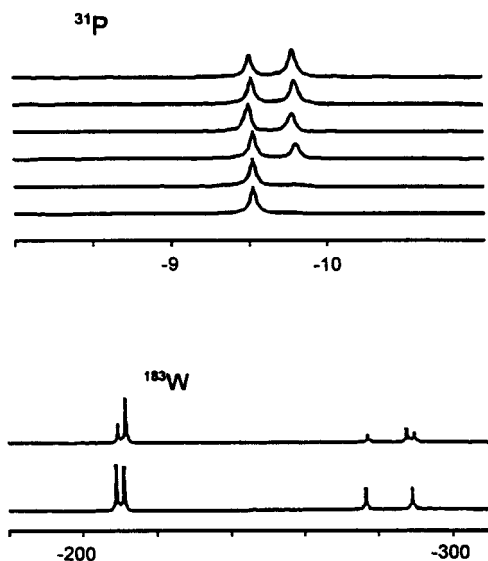


**Figure 8.** Top:  $^{31}\text{P}$  NMR spectra of  $[\text{Na}(\text{H}_2\text{O})\text{P}_5\text{W}_{30}\text{O}_{110}]^{14-}$  following hydrothermal treatment of solutions at pH 2 and in 0.1, 1, 2, 4, and 6 M HCl, from lower to upper respectively. Bottom:  $^{183}\text{W}$  NMR spectra of  $[\text{Na}(\text{H}_2\text{O})\text{P}_5\text{W}_{30}\text{O}_{110}]^{14-}$  before (lower) and after (upper) hydrothermal treatment in 2 M HCl (24 h at 170 °C).

**Na** (0.13 mmol) in 10 mL of 2 M HCl was found to contain 0.038 mmol of free, uncomplexed  $\text{Na}^+$  before hydrothermal treatment (170 °C, 24 h) and 0.095 mmol of  $\text{Na}^+$  after such treatment. Blank experiments with HCl showed no significant change of sodium activity upon hydrothermal treatment. The increase in  $\text{Na}^+$  activity corresponds to about 44% of the original heteropolyanion present, a value that is in agreement with the W NMR intensities (Figure 8) which indicate a 40% conversion from **Na** to the sodium-free anion, “[ $\text{P}_5\text{W}_{30}\text{O}_{110}$ ] $^{15-}$ ”. The exact

composition of the latter complex is not defined of course, but it is possible that the central cavity might accommodate *two* protons, one in the position indicated in Figure 4, and the other in place of the sodium cation, in addition to one or two water molecules.

**Conclusions.** The Preyssler heteropolytungstate anion  $[\text{NaP}_5\text{W}_{30}\text{O}_{110}]^{14-}$  and its derivatives with other encrypted metal cations are shown to contain a nonlabile internal water molecule coordinated to the central atom and lying on the anion’s virtual  $C_5$  axis. At low pH the anions are protonated at an oxygen atom within the central cavity of the anion and proton exchange between protonated and unprotonated anions is slow on the NMR time scale. The rate of proton/deuteron exchange on the internal water molecule of the anion incorporating  $\text{Eu}^{3+}$  in aqueous ( $\text{D}_2\text{O}$ ) solution has been measured by phosphorus-31 NMR spectroscopy. The central sodium cation of the Preyssler anion can be removed in strongly acid solutions, leading to an anion of  $D_{5h}$  symmetry.

**Acknowledgment.** We thank Professor Hyunsoo So, Sogang University, for drawing our attention to the additional signals in the  $^1\text{H}$  NMR spectrum of the europium derivative. This research has been supported by the Department of Energy through Grant No. DE-FG07-96ER14695. The purchase of the diffractometer was made possible by funds from NSF and Georgetown University.

**Supporting Information Available:** Table S1 (experimental data for Figure 5) and Table S2 (experimental data for Figure 7) (PDF). X-ray crystallographic files for **Na**, **Ca**, **HCa**, **Y**, **HY**, and **HU** are also available (CIF). This material is available free of charge via the Internet at <http://pubs.acs.org>.

JA992105B